13

Investigation of the composition of samarium monosulfide films obtained by electron beam heating

© E.B. Baskakov, V.I. Strelov

Shubnikov Institute of Crystallography „Crystallography and Photonics“ Russian Academy of Sciences,
119333 Moscow, Russia
e-mail: baskakov.ras@gmail.com

Received July 14, 2023
Revised September 26, 2023
Accepted September 26, 2023

The elemental composition of thin films obtained by electron beam heating of bulk SmS samples with a different element ratio: 1Sm : 1S, 1.05Sm : 1S and 1.15Sm : 1S. has been studied by energy dispersive spectroscopy. The analysis of elemental composition before and after spraying on the substrate was carried out on a volume sample of the composition 1.15Sm : 1S. According to the microanalysis data, a change in the content of elements was established and an assessment of the change in the phase composition in the sprayed material was made. It is shown that the composition of the obtained thin films contains an excessive Sm content. A method for determining the inhomogeneity of the composition in depth for SmS films is proposed, in which, using a two stream model of charged particle transport, the dependence of the electron beam path on the primary electron energy in SmS for energies up to 30 keV is calculated.

Keywords: electron beam heating, samarium monosulfide, energy dispersive X-ray analysis (EDAX), transport length of a monoenergetic electron beam in a sample.

DOI: 10.61011/TP.2023.11.57508.182-23

Introduction

Samarium monosulphide (SmS) is one of rare earth chalcogen elements that have been of interest with researchers for a long time [1,2] thanks to their properties which are relevant for various applications. In particular, SmS features low pressure of isostructural metal-semiconductor phase transition, i.e. 0.65 GPa at 300 K [3], high thermal stability with melting temperature about 2475 K [4], considerable thermo-emf ($\alpha \approx 170-350\,\mu$V/K [4–6]) and conductivity about $500\,\Omega^{-1}$/cm (at $T = 300$ K) for near-stoichiometric samples [4] high piezo- and tensoresistive effects (gauge factor $K \sim 40-50$ for polycrystalline films, $K \leq 260$ for single-crystals whose piezoresistance coefficient in hydrostatic compression is$\pi g \leq 6 \cdot 10^{-3}\,\mathrm{MPa}^{-1}$) [7,8]. In addition, SmS, like some semiconductors [9,10], has a quite promising property — thermovoltaic effect [11] that is defined at the possibility to generate electric current in heating without inducing a temperature gradient forcedly and is demonstrated in some papers [12–14].

Particular attention to thermovoltaic effect in SmS was caused by generated voltage. While heating up to 400–500 K without inducing external temperature gradients, the generated voltage achieved ~ 2.5 and ~ 4.5 V for single-crystal samples and thin films, respectively [15]. Besides high thermo-emfs, focus in made on thin film capability of forming SmS -based multilayer structures [16] to increase the generated voltage. The SmS film formation methods mainly include magnetron sputtering [12,17], explosive sputtering [18], ion-beam evaporation [19] and pulsed laser deposition [20]. The study [21] used the electron-beam heating or evaporation method to produce SmS films, where Sm metal served as the target material, for which it was sputtered in H_2S atmosphere (reactive sputtering). However, the electron-beam heating method allows to sputter refractory metals and compounds, its potential application for SmS sputtering to produce SmS thin films with pre-defined composition without H_2S is of interest.

The objective of the study was to investigate the capability of producing thin SmS films the electron-beam heating from bulk SmS samples and to define the composition of the prepared SmS films by the energy-dispersive spectroscopy method. Analysis of the prepared films was carried out using electron microscopy that has been well proven at the previous investigation stages of samarium monosulphide thin-film coatings applied by the magnetron sputtering method [22,23].

1. Materials and methods

The bulk SmS material used for sputtering by the electron-beam heating method consisted of three spherical granules 5 mm in diameter with various composition: 1Sm : 1S, 1.05Sm : 1S and 1.15Sm : 1S, that had been produced by ampoule synthesis from Sm and S [24]. Sm and S ratio in the granules was defined by different proportion of source materials involved in SmS synthesis. Excessive Sm concentration is provided in the source material to increase the concentration of impurity interstitial ions Sm^{2+} in the

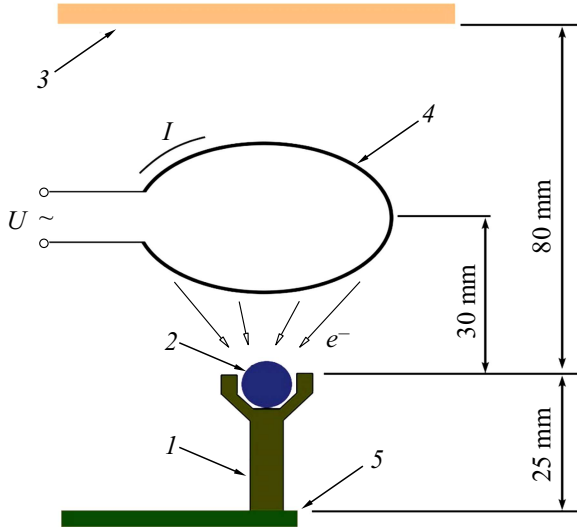

Figure 1. Electron-beam heating setup: *1* — graphite crucible, *2* — SmS granule, *3* — substrate, *4* — thermal cathode, *5* — crucible attachment/contact.

deposited films that is required to improve their thermo-emf [11]. Quantitative restrictions of Sm concentration in the samples are caused by the typical SmS homogeneity region that extends to 3.5 at.% of excess Sm [3], that corresponds to the source element ratio: 1.15Sm : 1S.

Bulk SmS samples were sputtered on polycrystalline glass St50 substrates using a graphite crucible on VUP-5 vacuum sputtering unit with preliminary evacuation of the vacuum chamber to $\sim 2 \cdot 10^{-4}$ Pa. The electron-beam heating setup used for the experiments is shown in Figure 1.

Sputtering process for each SmS sample with different phase composition was carried out as follows: SmS material *2* (Figure 1) was placed in graphite crucible *1*. Sputtering current up to 70 mA was set between thermal cathode contacts *4*. Between crucible contact *5* and cathode *4*, constant voltage about 4 kV was set to accelerate the electrons emitted by the thermal cathode. When the surface of the bulk SmS samples was bombarded by electrons, they were heated and SmS granules were further sputtered on substrate *3* during 10 min. The distance between the substrate and sputtered SmS was about 80 mm.

Chemical micro analysis of the bulk SmS material before and after sputtering and of the thin films was carried out by energy-dispersive spectroscopy using Jeol JCM−6000 PLUS scanning-electron microscope (SEM) complete with X-ray energy-dispersive spectrometer. Each of the deposited SmS films was examined in three points in the region above the center of the crucible during the sputtering process. The chemical analysis data contain average atomic fractures for each of the elements.

To define the monoenergetic electron beam path length in the substance (R_e) with normal particle setting onto the sample surface in SmS, double-stream model of charged particle transport in condensed substance with multiple scattering was used [25]. The model considered elastic and inelastic electron scattering. In case of SmS, when using moderate accelerating voltage of $E_0 < 30$ keV, the expression for R_e, [μm] may be written as:

$$R_e = E_0^2 \left(4\pi q^4 n_0 Z \ln(E_0^2/C_M^2)\right)^{-1}, \qquad (1)$$

where E_0 is the electron beam energy, [keV]; q is the electron charge, [C]; n_0 is the number of atoms per unit volume of the substance; Z is the effective atomic number; C_M is the universal constant equal to 790 eV.

2. Findings and discussion

Electron-beam heating is a process when kinetic energy of the accelerated electron flow bombarding the substance surface transforms into thermal energy resulting in substance heating up to the evaporation temperature [26,27], however, the composition of the deposited films in this case may differ from that of the source (sputtered) material [28]. When using the accelerating voltage of ~ 4 kV, it was assumed that intensive deposition of homogeneous SmS film is possible in case of congruous evaporation [29] with achievement of the SmS melting temperature equal to 2475 K. To check this assumption on the case of the initial sample with 1.15Sm : 1S, elemental analysis was carried out before and after sputtering. The investigation was carried out at the electron beam energy of 20 keV. The microanalysis data and estimated phase composition are shown in the Table.

Elemental analysis of the source material before sputtering (see the Table, Figure 2, *a*) has shown the presence of oxygen in it, that was due to the features of the SmS synthesis process [4] and surface oxidation in future [30]. However, oxygen in the SmS sample is usually within the Sm_2O_2S phase [30,31]. Assuming that full amount of oxygen is contained in the Sm_2O_2S phase, and the remaining Sm and S are contained within the $Sm_{1.15}S$ phase, the microanalysis data suggests that uncoupled Sm is present in the initial sample. The excessive uncoupled Sm has been also detected by SEM methods in the SmS samples prepared by the ampoule synthesis method [32].

The microanalysis of the 1.15Sm : 1S sample after sputtering (see the Table, Figure 2, *b*) demonstrates the decrease in Sm and S concentration in the compound with much more considerable decrease in the samarium fracture. The microanalysis also shows the increase in the oxygen fracture and carbon impurity. Similar to the chemical analysis of 1.15Sm : 1S before sputtering, it is likely that, for this sample after sputtering, the detected oxygen fracture is contained in the Sm_2O_2S phase. This means that 1.15Sm : 1S sputtering by the electron-beam heating results in full evaporation of the uncoupled Sm, decrease in the $Sm_{1.15}S$ phase concentration and formation of phases with excessive concentration of S, i.e. Sm_2S_3, Sm_3S_4 phases [4].

Increase in the oxygen content in the sample after sputtering is caused by oxidation of the 1.15Sm : 1S sample during heating that is apparently due to the presence of

Chemical analysis data for the sputtered 1.15Sm : 1S material and the estimated phase composition in the sample

Composition		Concentration in the material before sputtering, at.%	Concentration in the material after sputtering, at.%
Microanalysis	C	–	~ 9
	O	14	28
	S	34	27
	Sm	52	36
Estimated phase composition		$Sm_{1.15}S$, Sm_2O_2S, Sm	$Sm_{1.15}S$, Sm_2O_2S, Sm_2S_3, Sm_3S_4

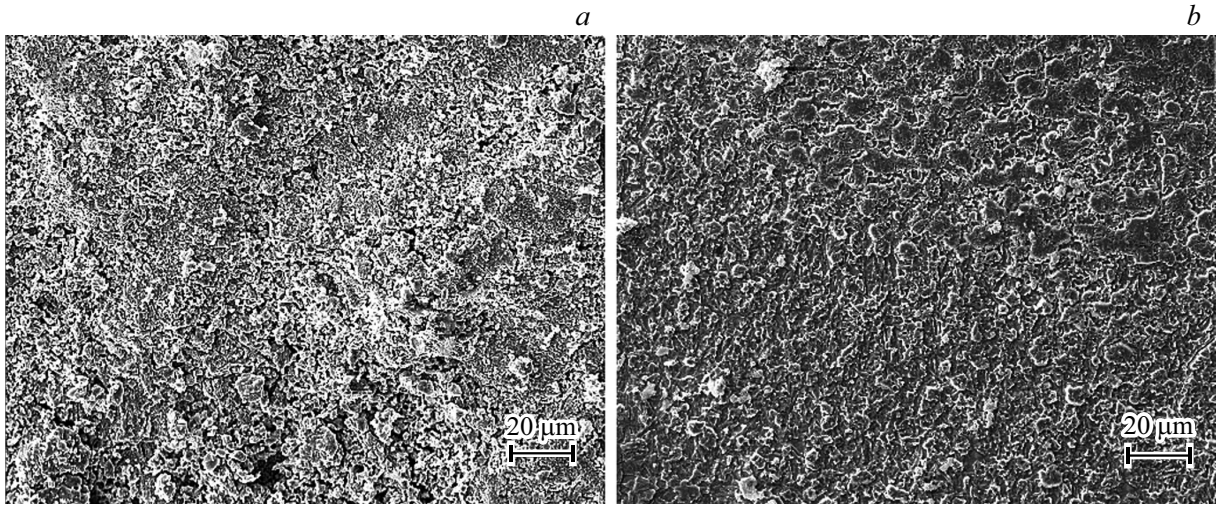

Figure 2. SEM images of the $Sm_{1.15}S$ surface: *a* — before sputtering, *b* — after sputtering.

oxygen in the residual atmosphere of the vacuum unit. This highlights the need to improve the sputtering process (improve vacuum in the chamber and provide additional crucible degassing).

The presence of carbon in the sample after sputtering is caused by partial evaporation of the crucible material (vacuum graphite sublimation) [33] where the initial 1.15Sm : 1S sample was placed. This is one of disadvantages of the electron-beam heating method when an uncooled crucible is used [34].

Thus, as shown by the microanalysis data, SmS sputtering results in the change in element concentrations in the sputtered sample, in particular, more intensive Sm sputtering from SmS takes place. This may suggest that excess Sm will be detected in the thin SmS films deposited by the electron-beam heating method, while concentration inhomogeneity will be observed in the film thickness. Sm concentration gradient in thin films may be used to improve the performance of SmS-based thermoelectric converters with high thermo-emf [16,35]. The change in the elemental composition in the film thickness may be assessed by SEM microanalysis of thin SmS films at various accelerating voltages, i.e. using the dependence of the maximum generation depth of the typical X-ray radiation in the sample on the accelerating voltage.

Using expression (1), a curve of electron path length in SmS vs. electron energy (Figure 3) was plotted.

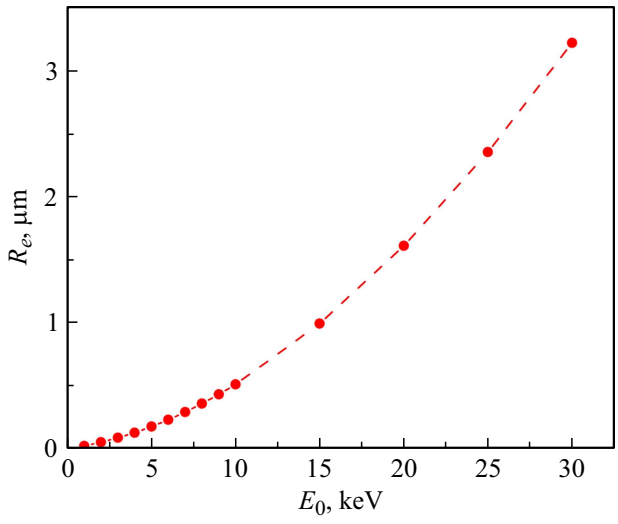

Figure 3. Dependence of the electron beam path length in SmS on the primary electron density.

The curve (Figure 3) shows that for electron beam microanalysis at E_0 5 and 20 keV, the typical X-ray radiation for SmS will be generated from a depth up to 0.18 and up to 1.6 μm, respectively. The microanalysis carried out at these energies will show the film material composition up to the corresponding thickness. Comparison of the film composition data at various energies suggests the distribution of the sputtered elements over the thickness of the deposited films.

Figure 4 shows the summarized microanalysis data containing the Sm to S concentration ratios for thin-film samples produced by sputtering 1Sm : 1S, 1.05Sm : 1S and 1.15Sm : 1S granules. In case of the film produced by 1Sm : 1S sputtering, the microanalysis at 20 keV did not provided quantitative assessment of the Sm and S concentrations in the films, because peaks from the substrate material prevailed in the spectrum. This suggests that the film thickness was lower than the electron beam path length at 20 keV, which corresponds to 1.6 μm. For microanalysis of thin films applied by 1.05Sm : 1S and 1.15Sm : 1S sputtering with the electron beam energy of 20 keV, peaks from the substrate material were observed in the spectrum, but the assay content of the detected substrate elements was lower than 1% suggesting that the thickness of these SmS films is $\geq$ 1.6 μm.

According to the film microanalysis data (Figure 4), the layer with thickness up to 0.18 μm has deficiency in Sm concentration with respect to S compared with the initial composition of the sputtered material. Microanalysis of films to a thickness up to 1.6 μm, the 1.05Sm : 1S and 1.15Sm : 1S samples show excessive Sm concentration with respect to S, that agrees with the decrease in Sm concentration in the microanalysis data for the initial sputtered material.

Microanalysis of thin SmS films deposited by sputtering 1.05Sm : 1S and 1.15Sm : 1S at a beam energy of 20 keV has shown that oxygen ($\sim$ 16%) and carbon ($\sim$ 11%) are present in them. Oxygen concentration in thin SmS films is comparable with that in the initial 1.15Sm : 1S material before sputtering, which confirms the presence of oxidation process mainly in the initial material during heating. Carbon content in thin SmS films corresponds to its content in the initial material after sputtering, which suggests that the

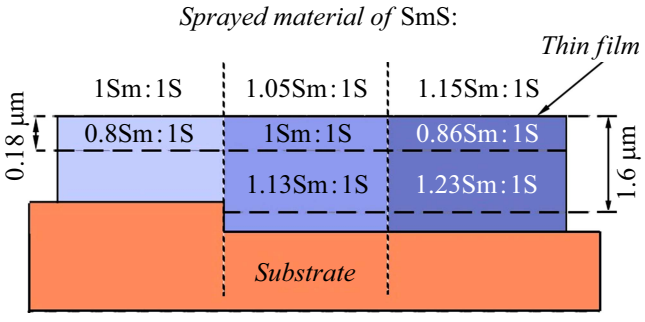

Figure 4. Elemental microanalysis data for SmS films deposited by sputtering SmS samples with various composition

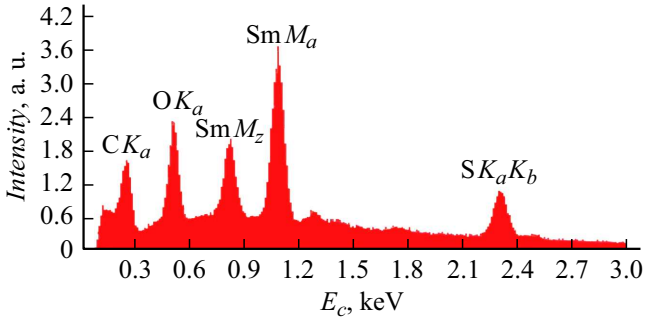

Figure 5. Characteristic radiation spectrum recorded in 1.15Sm : 1S sputtering.

crucible material enters both the source material and the film during 1.15Sm : 1S sputtering.

To define the degree of inhomogeneity of the film composition, consideration is given to the generation of energy-dispersive spectra by a heavy element contained in the compound. Since in samarium monosulphide for Sm and S, L_αSm ($E_c = 6.716$ keV) has the maximum excitation energy among the characteristic spectrum power intensity lines [36], the electron beam energy equal to 5 keV was not enough to detect this line during analysis of this compound (Figure 5).

Figure 5 shows energy-dispersive spectrum of the film deposited by sputtering 1.15Sm : 1S, where L_α-line from Sm is not detected. Therefore, the microanalysis of the layer with a thickness up to 0.18 μm shows deficiency in Sm concentration compared with its actual concentration.

Thus, the comparison of the quantitative microanalysis at $E_0 = 5$ and 20 keV has shown that, to determine the Sm and S concentration gradient in the SmS film thickness more accurately, energy-dispersive spectroscopy of thicker SmS films is required at the electron beam energies of $E_0 > 13.4$ keV to ensure reliable recording of Sm lines at $E_0/E_c > 2$ [37].

Conclusion

The study used electron beam heating of SmS samples with 1Sm : 1S, 1.05Sm : 1S and 1.15Sm : 1S to produce thin SmS films. Using SEM and energy-dispersive spectroscopy method, elemental composition variation was detected in the sputtered material for the 1.05Sm : 1S sample case. It was shown that more extensive Sm sputtering from the initial sample occurs during electron beam heating. It has been detected that excessive Sm concentration is present in the films deposited by 1.05Sm : 1S and 1.15Sm : 1S sputtering. Using the dependence of the depth of generation of characteristic X-ray radiation on the electron beam energy using the double-stream model of charged particle transport, electron beam path length in SmS was calculated for energies up to 30 keV.

Funding

The study was carried out under the state assignment FSRC„Crystallography and Photonics“ RAS using the equipment provided by SRC FSRC„Crystallography and Photonics“ RAS.

Conflict of interest

The authors declare that they have no conflict of interest.

References

[1] A.V. Golubkov, E.V. Goncharova, V.P. Zhuze, G.M. Loginov, V.M. Sergeeva, I.A. Smirnov. *Fizicheskie svoistva khalkogenidov RZE* (Nauka, L., 1973)
[2] A.V. Golubkov, V.M. Sergeeva. ZhVKhO, **2** (6), 645 (1981).(in Russian)
[3] R. Keller, G. Guntherodt, W.B. Holzapfel, M. Dietrich, F. Holtzberg. Solid State Commun., **29**, 753 (1979). DOI: 10.1016/0038-1098(79)90154-6
[4] O.V. Andreev, V.V. Ivanov, A.V. Gorshkov, P.V. Miodushevskiy, P.O. Andreev. Eurasian Chemico-Technol. J., **18** (1), 55 (2016). DOI: 10.18321/ectj396
[5] V.V. Kaminskii, A.A. Molodykh, I.S. Polukhin, S.M. Solov'ev, K.V. Shuraev. Tech. Phys. Lett., **40** (6), 453 (2014). DOI: 10.1134/S1063785014060066
[6] L. Li, S. Hirai, Y. Tasaki. J. Rare Earths, **34** (10), 1042 (2016). DOI: 10.1016/S1002-0721(16)60132-1
[7] V.V. Kaminskiy, N.N. Stepanov, A.A. Molodykh. Physics Solid State, **52** (7), 1356 (2010). DOI: 10.1134/S106378341007005X
[8] V.V. Kaminskiy, V.A. Sidorov, N.N. Stepanov, M.M. Kazanin, A.A. Molodykh, S.M. Solov'ev. Physics Solid State, **55** (2), 293 (2013) DOI: 10.1134/S106378341302011X
[9] I.A. Pronina, N.D. Yakushova, D.Ts. Dimitrov, L.K. Krasteva, K.I. Papazova, A.A. Karmanov, I.A. Averin, A.Ts. Georgieva, V.A. Moshnikov, E.I. Terukov. Tech. Phys. Lett., **43** (9), 825 (2017). DOI: 10.1134/S1063785017090255
[10] V.V. Kaminskii, S.M. Solov'ev, N.V. Sharenkova, S. Hirai, Y. Kubota. Tech. Phys. Lett., **44** (12), 1087 (2018). DOI: 10.1134/S106378501812026X
[11] M.M. Kazanin, V.V. Kaminskii, S.M. Solov'ev. Tech. Phys., **45** (5), 659 (2000). DOI: 10.1134/1.1259698
[12] V.I. Strelov, E.B. Baskakov, U.N. Bendryshev, V.M. Kanevskii. Crystallography Reports, **64** (2), 311 (2019). DOI: 10.1134/S1063774519020299
[13] V.M. Egorov, V.V. Kaminskii, M.M. Kazanin, S.M. Solov'ev, A.V. Golubkov. Tech. Phys. Lett., **41** (4),381 (2015). DOI: 10.1134/S1063785015040227
[14] V.V. Kaminskii, A.O. Lebedev, S.M. Solov'ev, N.V. Sharenkova. Tech. Phys., **64** (2), 181 (2019). DOI: 10.1134/S1063784219020075
[15] M.A. Grevtsev, G.D. Havrov, S.A. Kazakov, V.V. Kaminskii. J. Phys.: Conf. Series, **1038**, 012111 (2018). DOI: 10.1088/1742-6596/1038/1/012111
[16] V.V. Kaminskii, M.M. Kazanin. Tech. Phys. Lett., **34** (4), 361 (2008). DOI: 10.1134/S1063785008040263
[17] V.G. Bamburiv, O.V. Andreeve, V.V. Ivanov, A.N. Voropai, A.V. Gorshkov, A.A. Polovnokov, A.N. Bobylev. DAN **473** 6 (676) (in Russian).
[18] V.V. Kaminskii, M.M. Kazanin, S.M. Solov'ev, N.V. Sharenkova, N.M. Volodin. Semiconductors, **40** (6), 651 (2006). DOI: 10.1134/S1063782606060078]
[19] Yu.E. Kalinin, V.A. Makagonov, S.Yu. Pankov, A.V. Sitnikov, M.V. khakhlenkov. Vestn. Vor.gos.tekh.un-ta, **10** (6), 135 (2014).
[20] P.E. Teterin, A.V. Zenkevich, Yu.Yu. Lebedinsky, O.E. Parfenov. Trudy nauchnoy sessii MIFI, **3**, 172 (2010) (in Russian).
[21] E. Rogers, P.F. Smet, P. Dorenbos, D. Poelman, E. van der Kolk. J. Phys. Condens. Matter., **22**, 015005 (2010). DOI: 10.1088/0953-8984/22/1/015005
[22] V.I. Strelov, E.B. Baskakov, V.V. Artemov. *Tez. dokl. XXVIII Ross. konf. po elektronnoy microscopii* (Tchernogolovka, Rossiya, 2020), t. 3. s. 97 (in Russian).
[23] E.B. Baskakov, V.I. Strelov. Crystallography Reports, **66** (6), 1078 (2021). DOI: 10.1134/S1063774521060055
[24] A.S. Vysokikh, P.V. Miodushevsky, P.O. Andreev. Vestn. TGU, **5**, 179 (2011) (in Russian).
[25] N.N. Mikheev. J. Synch. Investig, **13** (4), 719 (2019). DOI: 10.1134/S1027451019040281
[26] V.P. Krivobokov, N.S. Sochugov, A.A. Soloviev. *Plazmennye pokrytiya (metody i oborudovanie).* (Izd-vo Tomskogo politekh. un-ta, Tomsk, 2007) (in Russian).
[27] B.A. Movchan, N.D. Tutov. Izvestiya Kurskogo gos. tekh. un-ta, **26** (1), 12 (2009) (in Russian).
[28] L.K. Markov, I.P. Smirnova, A.S. Pavlyuchenko, E.M. Arakcheeva, M.M. Kulagina. Semiconductors, **43** (11), 1521 (2009). DOI: 10.1134/S1063782609110219
[29] K.S.S. Harsha. *Principles of Physical Vapor Deposition of Thin Films* (Elsevier, Great Britain, 2006).
[30] A.S. Vysokikh, O.V. Andreev, L.A. Golovina. Vestnik tyumenskogo gos. un-ta, **3**, 124 (2007) (in Russian).
[31] A.S. Vysokikh. Avtoreph.diss. (Tyumen, Tyumensky gos.un-t, 2011)
[32] I.S. Volchkov, E.B. Baskakov, V.I. Strelov, V.M. Kanevskii. Tech. Phys. Lett., **45** (11), 1127 (2019). DOI: 10.1134/S1063785019110294
[33] S.A. Shchukarev. *Lektsii po obshchemu kursu khimii* (Izd-vo LGU, L., 1962) (in Russian)
[34] A. Ivanov, B. Smirnov. Nanoindustriya, **S** (36), 28 (2012) (in Russian).
[35] V.V. Kaminskii, V.A. Didik, M.M. Kazanin, M.V. Romanova, S.M. Solov'ev. Tech. Phys. Lett., **35** (21), 981 (2009). DOI: 10.1134/S1063785009110030
[36] L.I. Mirkin. *Spravochnik po rentgenostrukturnomu analizu polikristallov*, pod red.prof. Ya.S. Umanskogo (Gos.izd. Fizmatlit, M., 1961) (in Russian), s. 12.
[37] J. Goldstein, H. Yakowitz, D.E. Newbury, E. Lifshin, J.W. Colby, J.R. Coleman. *Practical Scanning Electron Microscopy* (Plenum Press, NY., 1975), p. 85.

Translated by Ego Translating